www.ijmer.in
INTERNATIONAL JOURNAL OF MULTIDISCIPLINARY EDUCATIONAL RESEARCH
ISSN:2277-7881; IMPACT FACTOR :6.514(2020); IC VALUE:5.16; ISI VALUE:2.286
Peer Reviewed and Refereed Journal:VOLUME:9, ISSUE:12(5), December:2020

ALIGNED MAGNETIC FIELDEFFECT ON CASSON FLUID FLOW OVER A NON-UNIFORM THICKNESSSTRETCHED SURFACE

B. Mahesh Reddy
Department of Mathematics, JNTUH College of Engineering Sultanpur, Sangareddy Dist., India

ABSTRACT

In the study, we inspect the impact of cross diffusion and aligned magnetic field on Casson fluid flow along a stretched surface of variable thickness. The differential equations explaining the flow situation have been transitioned with the succor of suited transfigurations. The solution of the problem is achieved by using bvp5c Matlab package. From the solution, it is perceived that the flow, temperature and concentration fields are affected by the sundry physical quantities. Results explored for the flow over a uniform and a non-uniform thickness surfaces. The influence of emerging parameters on the flow, energy and mass transport are discussed with graphical and tabular results. Results show that the thermal, flow and species boundary layers are uneven for the flow over a uniform and non-uniform thickness stretched surfaces.

Keywords: Cross diffusion; Casson fluid; Aligned magnetic field; Slendering sheet

INTRODUCTION:

The convective mass and heat transfer past a stretched surface plays an essential part in modern industries for intends of reliable apparatus. The researchers showing distinct fascination on mass and heat transfer in non-Newtonian flows because of its significance in the recent applications and technology in thermal engineering and in addition other astrophysical and geophysical studies. Rashidi et al. [1] analytically studied the thermal radiation effect on micropolar fluid flow between porous medium. Bhattacharya et al. [2] extended this work by considering the flow towards a porous shrinking surface. The mass and heat transfer in magnetohydrodynamic flow past a flat plate with heat source/sink was presented by Chamkha et al. [3]. MHD viscous flow past an infinite vertical plate with constant mass flux has been reported by Saravana et al. [4]. Alam et al. [5] illustrated the impacts of thermophoresis and variable suction on MHD mass and heat transfer flow towards an inclined plate with thermal radiation.

The effects of cross diffusion on chemically reacting MHD flow past a permeable stretched surface with Brownian motion and thermophoresis was numerically analyzed by Kandasamy et al. [6]. Unsteady liquid film flow of pseudo-plastic nanoliquid with viscous dissipation and variable thermal conductivity was studied by Lin et al. [7]. The analytical investigation of multi and single-phase models used for the reduction of nanofluid flow was studied by Turkyilmazoglu [8]. A chemical reaction and transpiration effect on magnetohydrodynamic flow over a wedge was theoretically investigated by Kandasamy et al. [9]. An analytical investigation for chemically reacting MHD flow towards a surface was proposed by Ouaf [10]. A variable temperature effect on mixed convection flow over a wedge was presented by Hossain et al. [11]. MHD flow and heat transfer over an isothermal sheet with chemical reaction effect was proposed by Kabeir et al. [12]. Chemical reaction and thermal radiation effects on MHD flow past a permeable stretched surface by considering suction was discussed by Mohankrishna et al. [13]. MHD viscous flow past an expanding surface was analytically studied by Turkyilmazoglu [14]. Sandeep and Sulochana [15] numerically studied the mixed convection micropolar fluid flow towards an expanding/contracting surface with non-uniform heat source/sink.

MHD heat transfer flow of a non-Newtonian fluid past a shrinking surface was numerically explained by Akbar et al. [16]. A theoretical investigation on heat transfer and Carreau liquid flow was done by Jenny [17]. Mixed convection flow over a rotating cone was numerically studied by Anilkumar and Roy [18]. A new buoyancy induced model of Al-water nanofluid over a parabolic region was numerically studied by Sandeep and Animasaun [19]. Further, they extended their work by considering the flow over a stagnation region [20]. Chankha et al. [21] discussed the effect of thermal radiation on the flow over a wedge filled with porous medium. Cross diffusion effects on the MHD non-Newtonian fluid flows over a parabolic region was presented by Kumaran and Sandeep [22]. Koriko et al. [23] studied the flow over upper flat surface of a paraboloid of revolution with of Brownian motion and thermophoresis. Very recently, the reserchers [24, 25, 26] investigated the MHD flow over various flow geometries by considering the thermal radiation and Cattenao-Christov heat flux.

By keeping the above references in view, In this paper, we inspect the impact of cross diffusion and aligned magnetic field on magneto hydrodynamic Casson fluid. The flow is considered beside a stretched surface of variable thickness. The governing partial differential equations of the flow, heat and mass transfer are transformed into ODE's equations solved numerically by using bvp5c Matlab package. From the solution, it is perceived that the flow, concentration and temperature fields are affected by the sundry physical quantities.

A steady 2D flow of magnetohydrodynamic Casson fluid over a slendering stretched sheet is considered. The x-axis is considered along the sheet and the y-axis is perpendicular to it. It is supposed that $y = A(x+b)^{\frac{1-m}{2}}$, $u_w(x) = (x+b)^m U_{o,}\, v_w = o$, $m \neq 1$. This study induced magnetic field is neglected. Combined influence of Soret and Dufour impacts are considered. An aligned magnetic field of strength B_0 is employed as depicted in Fig.1 at different angles. In this study, $m \neq 1$ deals with the slendering sheet and m= 1 deals with the uniform thickness sheet.
With the above assumptions, the governing equations can be expressed as (refer [27]

$$\frac{\partial u}{\partial x} + \frac{\partial u}{\partial y} = 0, \qquad (1)$$

$$u\frac{\partial u}{\partial x} + v\frac{\partial u}{\partial y} = \nu\left(1 + \frac{1}{\beta}\right)\frac{\partial^2 u}{\partial y^2} - \frac{\sigma B^2(x) sin^2\alpha}{\rho}u, \qquad (2)$$

$$u\frac{\partial T}{\partial x} + v\frac{\partial T}{\partial y} = \frac{k}{\rho C_p}\frac{\partial^2 T}{\partial y^2} + \frac{D_m k_T}{C_s C_p}\frac{\partial^2 C}{\partial y^2}, \qquad (3)$$

$$u\frac{\partial C}{\partial x} + v\frac{\partial C}{\partial y} = D_m\frac{\partial^2 C}{\partial y^2} + \frac{D_m k_T}{T_m}\frac{\partial^2 T}{\partial y^2}, \qquad (4)$$

with the conditions

$$\left.\begin{aligned} &u = U_w(x) + h_1^* \left(\frac{\partial u}{\partial y}\right), v = 0, \\ &T = T_w\,(x) + h_2^* \left(\frac{\partial T}{\partial y}\right), C = C_w\,(x) + h_3^* \left(\frac{\partial C}{\partial y}\right) \\ &and \\ &u(\infty) = 0, T(\infty) = T_\infty, C(\infty) = C_\infty \end{aligned}\right\} \quad (5)$$

where

$$h_1^* = \left[\frac{2-f_1}{f_1}\right] \xi_1 (x+b)^{\frac{1-m}{2}}, \quad (6)$$

$$h_2^* = \left[\frac{2-a}{a}\right] \xi_2 (x+b)^{\frac{1-m}{2}}, \quad (7)$$

$$h_3^* = \left[\frac{2-d}{d}\right] \xi_3 (x+b)^{\frac{1-m}{2}}, \quad (8)$$

$$T_W - T_\infty = T_0 (x+b)^{\frac{1-m}{2}} \quad (9)$$

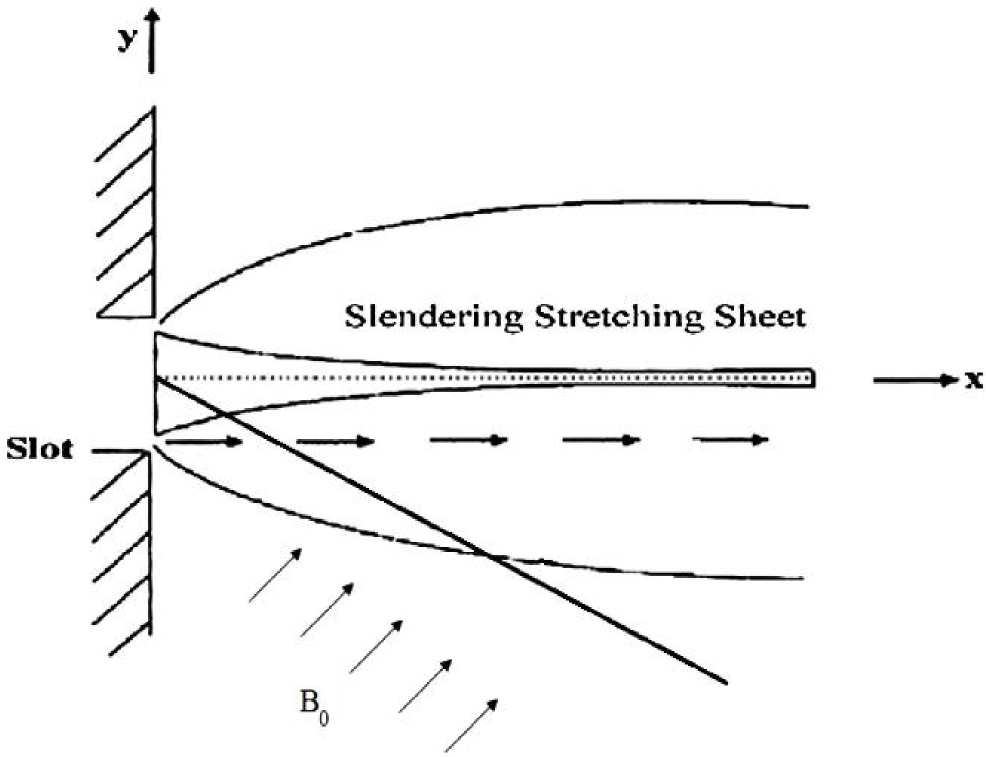

Fig. 1: Physical Model

we now suggest the following similarity transformations:

$$\psi = f(\eta)\left(\frac{2}{m+1}\nu U_0(x+b)^{m+1}\right)^{0.5} \quad (10)$$

$$\eta = y\left(\frac{m+1}{2}U_0\frac{(x+b)^{m-1}}{\upsilon}\right)^{0.5}, \quad (11)$$

$$\theta(T_w(x) - T_\infty) - T_\infty = T \quad (12)$$

If stream function ψ be described as $u = \frac{\partial\psi}{\partial y}$ and $v = -\frac{\partial\psi}{\partial x}$

$$u = U_0(x+b)^m f'(\eta) \quad (13)$$

with the help of (12), (13), equations (2)-(4) converted as

$$\left(1+\beta^{-1}\right)f''' + f''f - \frac{2m}{m+1}f'^2 - Msin^2\alpha f' = 0, \quad (14)$$

$$\theta'' + \Pr f\theta' + \Pr Du\phi'' - \Pr\frac{1-m}{m+1}f'\theta = 0, \quad (15)$$

$$\phi'' - Sc\frac{1-m}{m+1}f'\phi + Scf\phi' + ScSr\theta'' = 0, \quad (16)$$

and the corresponding conditions are

$$\left.\begin{aligned} &f(0) = \lambda\left(\tfrac{1-m}{m+1}\right)\left[1 + h_1 f''(0)\right], f'(0) = \left[1 + h_1 f''(0)\right], \\ &\theta(0) = \left[1 + h_2\theta'(0)\right], \phi(0) = \left[1 + h_3\phi'(0)\right], \\ &f' = 0, \theta = 0, \phi = 0 \quad as \quad \eta \to \infty \end{aligned}\right\} \quad (17)$$

where $\Lambda, M,$ Pr, Du, Sc, Sr are defined as

$$\left.\begin{aligned} &\Lambda = \Gamma\sqrt{(x+b)^{3m-1}\nu^{-1}(m+1)U_0^3}, \\ &M = \frac{2\sigma B_0^2}{\rho U_0(m+1)}, \Pr = \frac{\mu C_p}{k}, Du = \frac{D_m k_T(C_w - C_\infty)}{\nu C_s C_p(T_w - T_\infty)}, \\ &Sc = \frac{\nu}{D_m}, Sr = \frac{D_m k_T(T_w - T_\infty)}{\nu T_m(C_w - C_\infty)} \end{aligned}\right\} \quad (18)$$

The physical quantities of engineering interest, the friction factor, local Nusselt and Sherwood numbers are given by $C_f = 2\frac{\mu\frac{\partial u}{\partial y}}{\rho U_w^2}$

$$Sh_x = \frac{(x+d)\frac{\partial C}{\partial y}}{Cw(x) - C_\infty} \quad (19)$$

B$Nu_x = \frac{(x+b)\frac{\partial T}{\partial y}}{T_w(x) - T_\infty}$y using (5), (19) becomes

$$\left.\begin{aligned} &C_f(\mathrm{Re}_x)^{0.5} = 2\left(\tfrac{m+1}{2}\right)^{0.5}\left(\left(1+\beta^{-1}\right)f''(0) + \Lambda f''^2(0)\right), \\ &Nu_x = -\left(\tfrac{m+1}{2}\right)^{0.5}(\mathrm{Re}_x)^{0.5}\theta'(0), \\ &\mathrm{Sh}_x = -\left(\tfrac{m+1}{2}\right)^{0.5}(\mathrm{Re}_x)^{0.5}\phi'(0) \end{aligned}\right\} \quad (20)$$

Where $\mathrm{Re}_x = \frac{U_w X}{\nu}$ and $X = (x+b)$

DISCUSSION OF THE RESULTS

The set of ODEs (14)-(16) with the conditions (17) is numerically solved by employing bvp5c technique. For computational purposes, the pertinent parameter values considered as $Sc = 0.2$, $Pr = 6$, $\beta = 0.5$, $M = 3$, $Sr = 0.3$, $\gamma = \pi/3$, $h_1 = h_2 = h_3 = 0.5$, $Du = 0.2$, $\lambda = 0.2$. These values are kept as common in the entire study exclude the varied values as shown in respective tables and figures.

Figs. 2-4 explored the impact of M on velocity, temperature and concentration distributions of the flow over a variable and uniform thickness stretched surfaces. We observed that the increasing values of the Msuppresses the velocity field and boost the concentration and thermal fields in both cases. It is also observed that the influence of the M is large on the flow past a uniform thickness sheet when compared to variable thickness sheet. Physically, rising values of the M develop the negative force to the flow field known as Lorentz force. This leads to decline the velocity boundary layer thickness. The similar results have been observed in Figs. 5-7 for rising values of the aligned angle. This may be due to the fact that the increasing the aligned angle, strengthen the M hence develop the resistive force.

The impacts of Soret number on thermal and concentration fields are depicted in Figs. 8 and 9. It is clear that the boosting value of Sr enhances both the concentration and temperature fields. But we noticed an opposite trend to above in the concentration field for improving values of the Dufour number (See Figs. 10 and 11). Physically, the Soret and Dufour effects are a combined effect, which regulates the concentration and thermal fields. The effects of Casson parameter on concentration and temperature fields are depicted in Figs. 12 and 13. It is observed that the increasing value of the Casson parameter enhances the concentration and temperature fields in both cases. Generally, increasing values of the Casson parameter reduce the viscous nature of the flow field. This leads to increase the temperature and mass fields.

The effects of dimensionless velocity slip parameter on $f'(\eta)$, $\theta(\eta)$ and $\phi(\eta)$ fields are shown in Figs. 14-16. It is clear that the increasing value of velocity slip parameter decline $f'(\eta)$ and boosts the. It is evident from Figs. 15 and 16 that the slip influence is highly on $\theta(\eta)$ and. The impact of concentration and temperature slip parameters of thermal and concentration fields is depicted in Figs. 17-20. It is clear that the increasing values of h_2 and h_3 depreciate both $\theta(\eta)$ and $\phi(\eta)$ fields in both cases.

Numerical Procedure (bvp5c)

Bvp5c is a one of the boundary value problem solver in Matlab package. The bvp5c function is used exactly like bvp4c, with the exception of the meaning of error tolerances between the two solvers. If S(x) approximates the solution y(x), bvp4c controls the residual |S′(x)–f(x, S(x))|. This controls indirectly the true error |y(x)–S(x)|. bvp5c controls the true error directly.

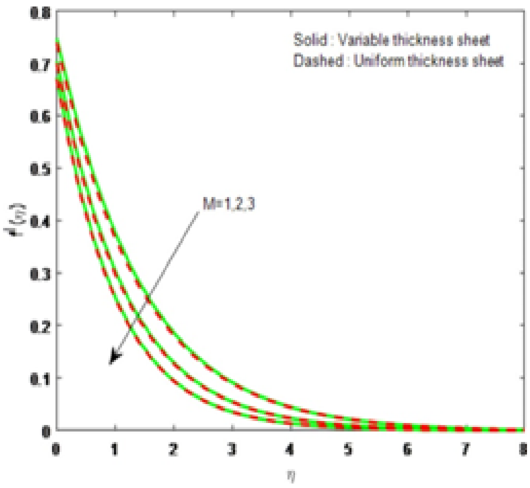

Fig. 2: Influence of M on velocity field

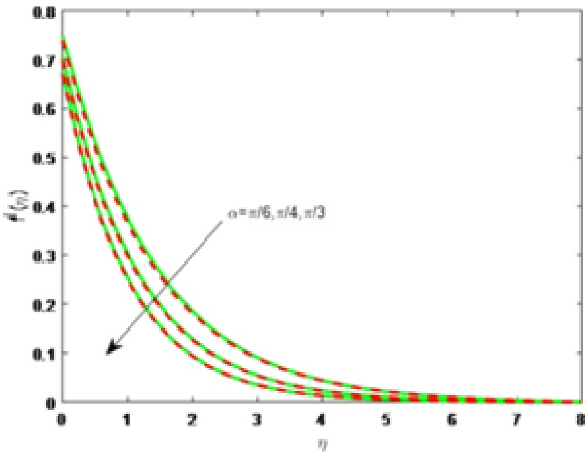

Fig. 5: Influence of α on velocity field

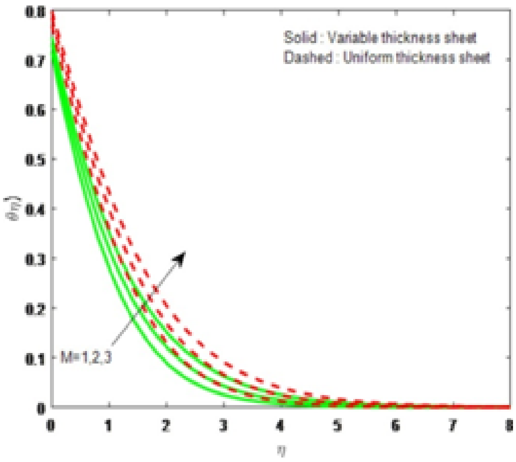

Fig. 3: Influence of M on temperature field

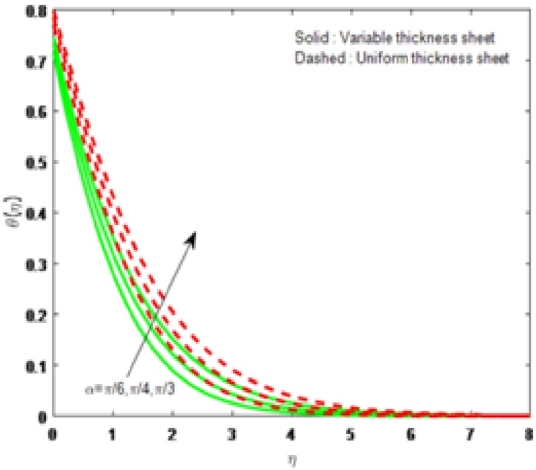

Fig. 6: Influence of α on temperature field

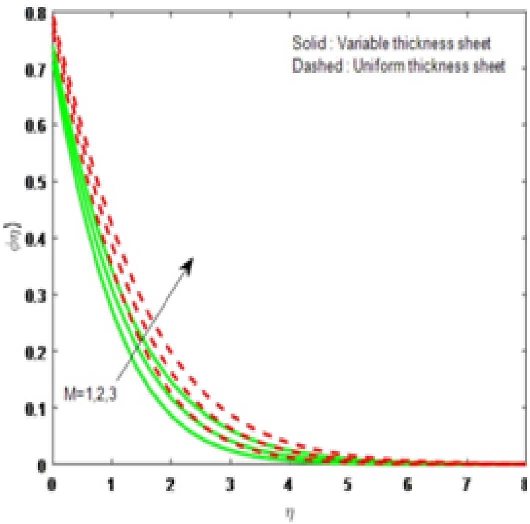

Fig. 4: Influence of M on concentration field

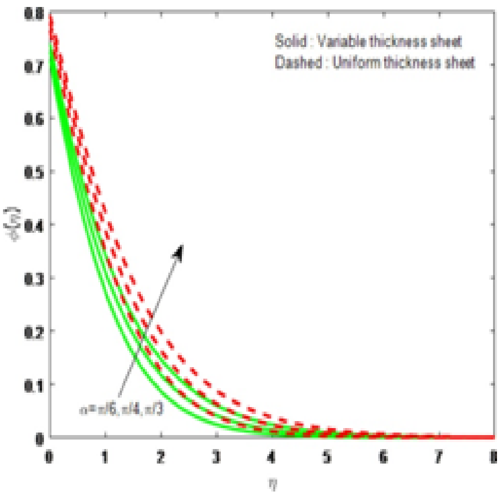

Fig. 7: Influence of α on concentration field

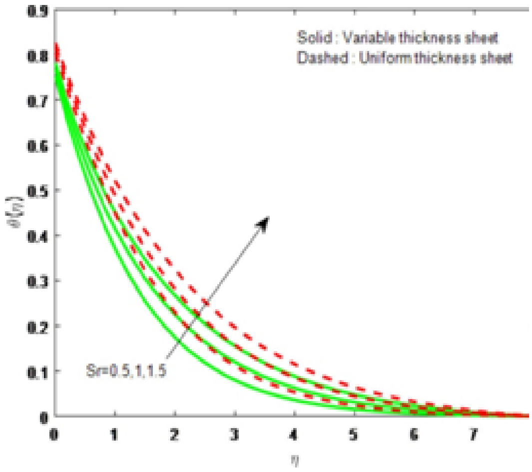

Fig. 8: Influence of Sr on temperature field

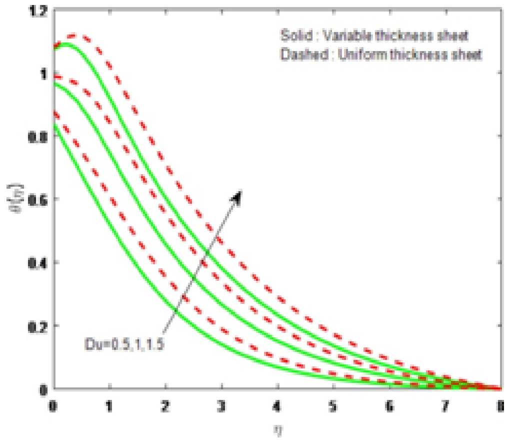

Fig. 10: Influence of Du on temperature field

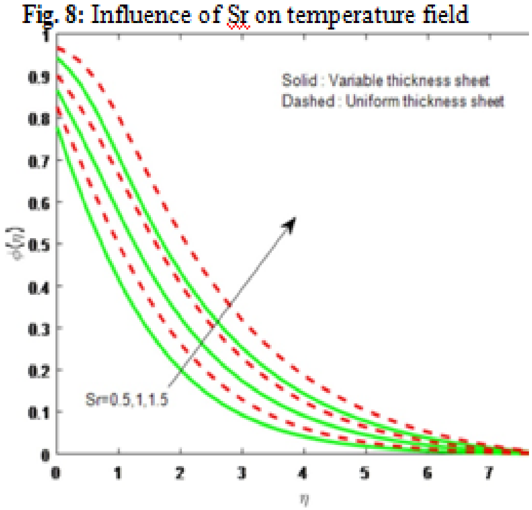

Fig. 9: Influence of Sr on concentration field

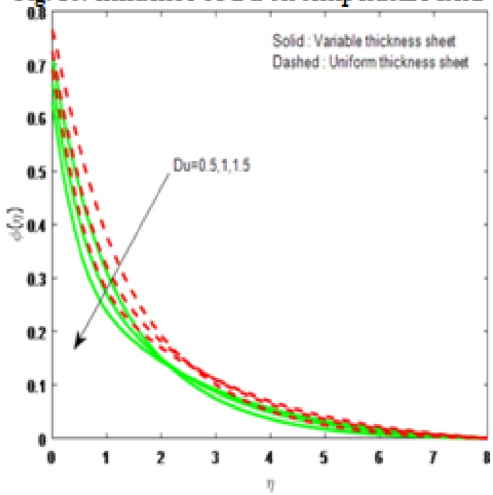

Fig. 11: Influence of Du on concentration field

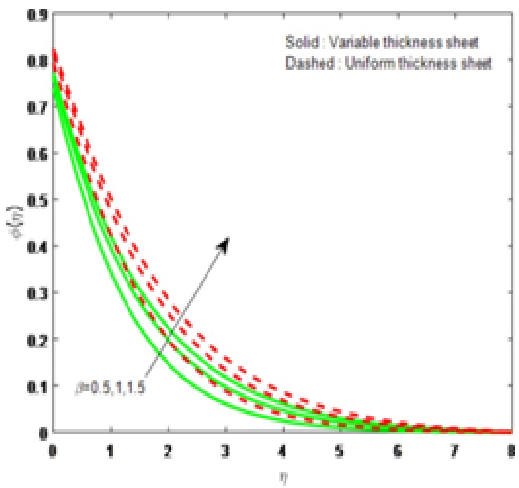

Fig. 12: Influence of β on temperature field

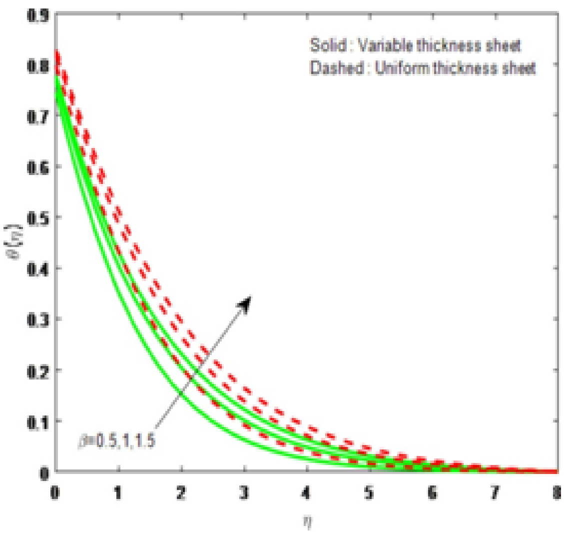

Fig. 13: Influence of β on concentration field

www.ijmer.in

INTERNATIONAL JOURNAL OF MULTIDISCIPLINARY EDUCATIONAL RESEARCH
ISSN:2277-7881; IMPACT FACTOR :6.514(2020); IC VALUE:5.16; ISI VALUE:2.286
Peer Reviewed and Refereed Journal:VOLUME:9, ISSUE:12(5), December:2020

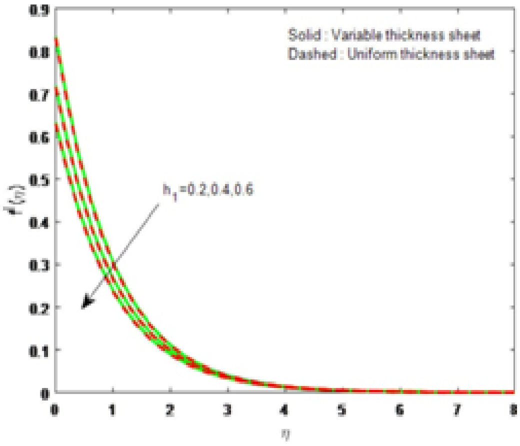

Fig. 14: Influence of h_1 on velocity field

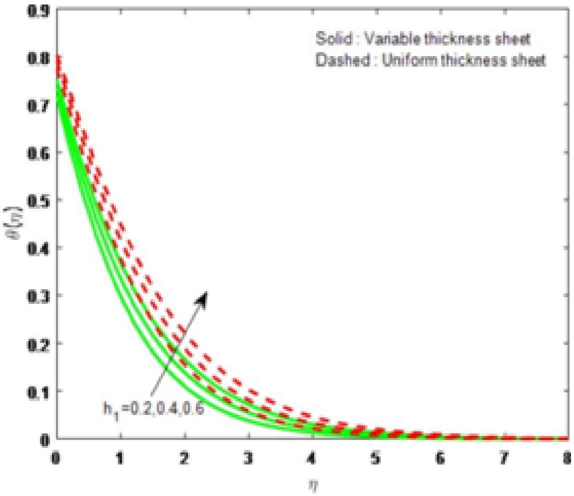

Fig. 15: Influence of h_1 on temperature field

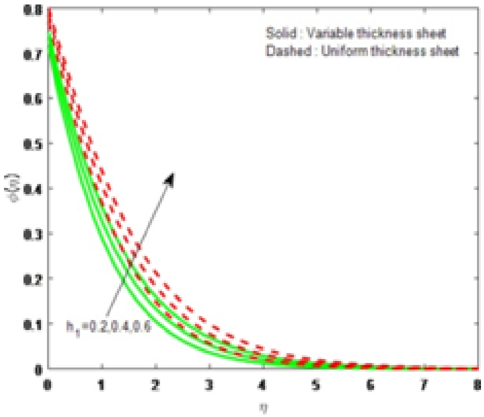

Fig. 16: Influence of h_1 on concentration field

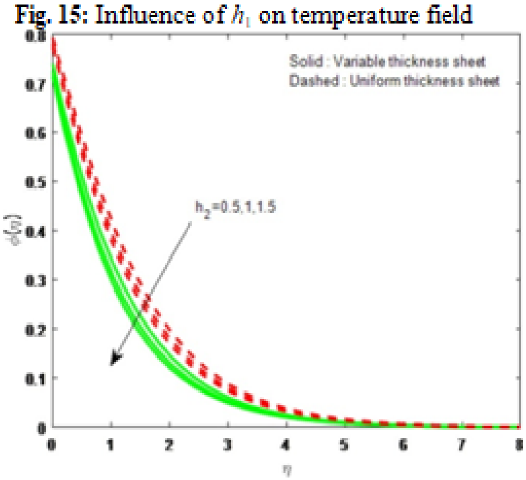

Fig. 18: Influence of h_2 on concentration field

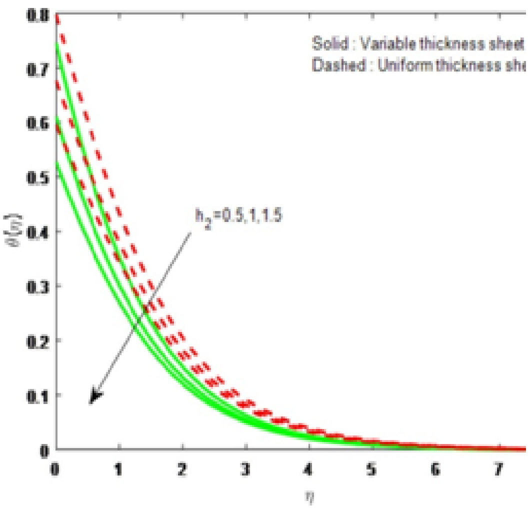

Fig. 17: Influence of h_2 on temperature field

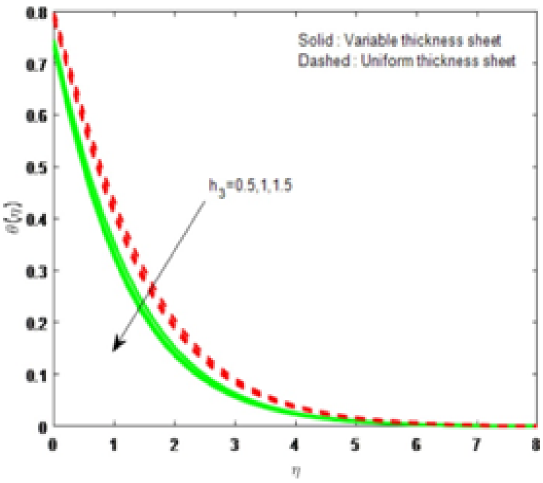

Fig. 19: Influence of h_3 on temperature field

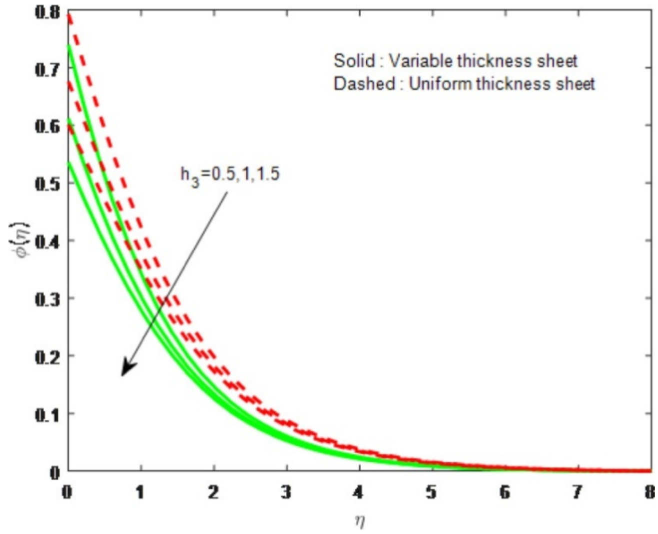

Fig. 20: Influence of h_3 on concentration field

Tables 1 and 2 shows the variation in the wall friction, reduced Nusselt and Sherwood numbers at different pertinent parameters. It is clear that the increasing values of M, α, Sr, β and h_1 suppresses the mass and heat transfer rate of the flows past a uniform and variable thickness stretching sheets. Increasing values of the Dufour number and temperature slip parameter declines Nusselt number and enhances the Sherwood number. But concentration slip parameter shows the opposite trend to the above. Varying values of the Soret, Dufour numbers, velocity and temperature slips is not showing a significant influence on wall friction, while M have tendency to decline the skin friction coefficient. Table3.Shows the validation of numerical technique with the Newtonian fluid.

Table 1: Variations in physical quantities for the flow over a variable thickness sheet

M	Sr	Du	α^0	β	h_1	h_2	h_3	C_f	Nu_x	Sh_x
1								−0.505140	0.495539	0.582760
2								−0.588985	0.466246	0.549117
3								−0.652936	0.441628	0.520833
	0.5							−0.652936	0.429327	0.442860
	1.0							−0.652936	0.402005	0.266693
	1.5							−0.652936	0.378817	0.113314
		0.5						−0.652936	0.282406	0.581449
		1.0						−0.652936	0.058035	0.668925
		1.5						−0.652936	−0.126725	0.743023
			30					−0.505140	0.495539	0.582760
			45					−0.588985	0.466246	0.549117
			60					−0.652936	0.441628	0.520833
				0.5				−0.652936	0.441628	0.520833
				1.0				−0.742597	0.403642	0.477147
				1.5				−0.784471	0.384937	0.455596
					0.2			−0.828335	0.488521	0.575301
					0.4			−0.702013	0.455775	0.537274
					0.6			−0.610565	0.428658	0.505754
						0.5		−0.652936	0.441628	0.520833
						1.0		−0.652936	0.337275	0.552628
						1.5		−0.652936	0.272812	0.572269
							0.5	−0.652936	0.441628	0.520833
							1.0	−0.652936	0.459920	0.388086
							1.5	−0.652936	0.470782	0.309263

Table 2Variations in physical quantities for the flow over a uniform thickness sheet

M	Sr	Du	α^o	β	h_1	h_2	h_3	C_f	Nu_x	Sh_x
1								-0.521103	0.462819	0.472203
2								-0.599633	0.431194	0.440696
3								-0.660650	0.404706	0.414282
	0.5							-0.660650	0.393374	0.346888
	1.0							-0.660650	0.368633	0.195334
	1.5							-0.660650	0.348083	0.064136
		0.5						-0.660650	0.245853	0.470118
		1.0						-0.660650	0.023572	0.550903
		1.5						-0.660650	-0.158344	0.619420
			30					-0.521103	0.462819	0.472203
			45					-0.599633	0.431194	0.440696
			60					-0.660650	0.404706	0.414282
				0.5				-0.660650	0.404706	0.414282
				1.0				-0.749609	0.363967	0.373563
				1.5				-0.791064	0.344614	0.354158
					0.2			-0.842679	0.450978	0.460942
					0.4			-0.711336	0.418563	0.428264
					0.6			-0.617033	0.392084	0.401538
						0.5		-0.660650	0.404706	0.414282
						1.0		-0.660650	0.323705	0.437529
						1.5		-0.660650	0.269721	0.453023
							0.5	-0.660650	0.404706	0.414282
							1.0	-0.660650	0.420215	0.323921
							1.5	-0.660650	0.430170	0.265920

Table 3**Validation of the results of $f''(0)$ with Ref. [26] for Newtonain Case**

λ	h_1	Ref. [26]	Present Results
0.2	0	−0.924828	−0.9248291230
0.25	0.2	−0.733395	−0.7333964851
0.5	0.2	−0.759570	−0.7595702140

The influence of cross diffusion and aligned magnetic field on magnetohydrodynamic Casson fluid is investigated theoretically along a stretched surface of variable thickness. The differential equations explaining the flow situation have been transitioned with the succor of suited transfigurations. The solution of the problem is achieved by using bvp5c Matlab package. From the solution, it is perceived that the flow, temperature and concentration fields are affected by the sundry physical quantities. Results explored for the flow over a uniform and a non-uniform thickness surfaces. The numerical observations are as follows:

1. The thermal and concentration boundary thicknesses are non-uniform for the flow over a uniform and variable thickness stretched surfaces.
2. The heat and mass transfer rate is high in the flow over a variable thickness surface when compared to the uniform thickness surface.
3. Aligned magnetic field regulates the flow, thermal and concentration fields.
4. Casson parameter has tended to decline the heat and mass transfer rate.
5. Cross diffusion regulates the temperature and concentration fields.
6. Slip parameters monitor the heat and mass transfer performance.

Nomenclature

u, v	Velocity components in *x*and*y*directions (m/s)
x	Direction along the surface (m)
y	Direction normal to the surface (m)
C_p	Specific heat capacity at constant pressure (J/kg K)
f	Dimensionless velocity
A	constant related to stretching sheet
$B(x)$	Magnetic field parameter (kg/s^2 A)
T	Temperature of the fluid (K)
k	Thermal conductivity (W/m K)
D_m	Molecular diffusivity of the species concentration (m^2/s)
k_T	Thermal diffusion ratio (m^2/s)
C_s	Concentration susceptibility
C	Concentration of the fluid (mol/m^3)
T_m	Mean fluid temperature (K)
T_∞	Temperature of the fluid in the free stream (K)
C_∞	Concentration of the fluid in the free stream (K)
h1∗	Dimensional velocity slip parameter
h2∗	Dimensional temperature jump parameter
h3∗	Dimensional concentration jump parameter
a	Thermal accommodation coefficient
b	Physical parameter related to stretching sheet
d	Concentration accommodation coefficient
m	Velocity power index parameter
Pr	Prandtl number
M	Magnetic interaction parameter
Du	Dufour number
Sc	Schmidt number
Sr	Soret number
h_1	Dimensionless velocity slip parameter
h_2	Dimensionless temperature jump parameter

h_3 Dimensionless concentration jump parameter

C_f Skin friction coefficient

Nu_x Local Nusselt number

Sh_x Local Sherwood number

Re_x Local Reynolds number

Greek Symbols

ϕ Dimensionless concentration

η Similarity variable

σ Electrical conductivity of the fluid (S/m)

γ Ratio of specific heats

θ Dimensionless temperature

ρ Density of the fluid (kg/m^3)

β Casson fluid parameter

μ Dynamic viscosity (Pa s)

υ Kinematic viscosity (m^2/s)

λ Wall thickness parameter

ξ_1 Mean free path (constant)

α Aligned angle

References

1. M. M. Rashidi, S. A. Mohimanian pours, S. Abbasbandy, Analytic approximate solutions for heat transfer of a micropolar fluid through a porous medium with radiation. Commun. Nonlinear Sci. Numer. Simulat. 16 (2011) 1874-1881.
2. K. Bhattacharyya, S. Mukhopadhyay, G.C. Layek, I. Pop, Effects of Thermal Radiation On Micropolar Fluid Flow and Heat Transfer over a Porous Shrinking Sheet, Int. J. Heat Mass Transfer, 55 (2012) 2945-2952.
3. A.J. Chamkha, C. Issa, Effects of heat generation/absorption and thermophoresis on hydromagnetic flow with heat and mass transfer over a flat surface, International Journal of Numerical Methods for Heat & Fluid Flow, 10 (4), 2000, 432-449.
4. R. Saravana, S. Sreekanth, S. Sreenadh, R. Hemadri Reddy, Mass transfer effects on MHD viscous flow past an impulsively started infinite vertical plate with constant mass flux, Advances in Applied Science Research, 2(1) (2011) 221-229.
5. M.S. Alam, M.M. Rahman, M.A. Sattar, Effects of variable suction and thermophoresis on steady MHD combined free-forced convective heat and mass transfer flow over a semi-infinite permeable inclined plate in the presence of thermal radiation, International Journal of Thermal Sciences, 47, 2008, 758-765.

6. R. Kandasamy, T. Hayat, S. Obaidat, Group theory transformation for Soret an Dufour effects on free convective heat and mass transfer with thermophoresis and chemical reaction over a porous stretching surface in the presence of heat source/sink, Nuclear Engineering and Design, 241, 2011, 2155-2161.
7. Y. Lin, L. Zheng, G. Chen, Unsteady flow and heat transfer of pseudo-plastic nanoliquid in a finite thin film on a stretching surface with variable thermal conductivity and viscous dissipation, Powder Technol. 274 (2015) 324–332. .
8. M. Turkyilmazoglu, Analytical solutions of single and multi-phase models for the condensation of nanofluid film flow and heat transfer, Eur. J. Mech. B/Fluids. 53 (2015) 272–277. .
9. R. Kandasamy, K. Periasamy, K.K.S. Prabhu, Effects of chemical reaction, heat and mass transfer along a wedge with heat source and concentration in the presence of suction or injection, Int. J. Heat Mass Transf. 48 (7) (2005) 1388-1394.
10. M.E. Ouaf, Exact solution of thermal radiation on MHD flow over a stretching porous sheet, Appl. Math. Comp. 170 (2) (2005) 1117-1125.
11. M.A. Hossain, S. Bhowmick, R.S.R. Gorla, Unsteady mixed-convection boundary layer flow along a symmetric wedge with variable surface temperature, Int. J. Eng. Sci. 44 (10) (2006) 607-620.
12. S.M.M. El-Kabeir, M. Modather, M. Abdou, Chemical reaction, heat and mass transfer on MHD flow over a vertical isothermal cone surface in micropolar fluids with heat generation/absorption, Appl. Math. Sci. 1 (34) (2007) 1663-1674.
13. P. Mohan Krishna, N.Sandeep, V.Sugunamma. Effects of radiation and chemical reaction on MHD convective flow over a permeable stretching surface with suction and heat generation. Walaliak Journal of Science and Technology Walailak J Sci& Tech 12(9) (2015) 831-847.
14. Turkyilmazoglu M. Analytic heat and mass transfer of the mixed hydrodynamic/thermal slip MHD viscous flow over a stretching sheet. Int J MechSci 53(10) (2011) 886–96.
15. N.Sandeep, C.Sulochana, Dual solutions for unsteady mixed convection flow of MHD Micropolar fluid over a stretching/shrinking sheet with non-uniform heat source/sink. Engineering Science and Technology, an International Journal 18 (2015) 738-745.
16. Akbar NS, Nadeem S, UI Haq R, Ye S (2014). MHD stagnation point flow of Carreau fluid toward a permeable shrinking sheet: Dual solutions. Ain Shams Eng J, 5, 1233-1239.
17. Jenny M, Plaut E, Briard A (2015). Numerical study of subcritical Rayleigh-Benard convection rolls in strong shear thinning Carreau fluids. J Non-Newtonian Fluid Mech, 219, 19-34.
18. Anilkumar D, Roy S (1963). Unsteady mixed convection flow on a rotationg cone in rotating fluid. Appl Math Computation, 155, 545-561.
19. I.L.Animasaun, N.Sandeep, Buoyancy induced model for the flow of 36nm alumina-water nanofluid along upper horizontal surface of a paraboloid of revolution with variable thermal conductivity and viscosity, Powder Technology, 301 (2016) 858-867.
20. N. Sandeep, O.K. Koriko, I.L. Animasaun, Modified kinematic viscosity model for 3D-Casson fluid flow within boundary layer formed on a surface at absolute zero, Journal of Molecular Liquids, 221 (2016) 1197–1206.
21. A.J. Chamkha, S. Abbasbandy, A.M. Rashad, K. Vajravelu, Radiation Effects on Mixed Convection over a Wedge Embedded in a Porous Medium Filled with a Nanofluid, Transport in Porous Media. 91 (2012) 261–279.
22. G.Kumaran, N.Sandeep, Thermophoresis and Brownian moment effects on parabolic flow of MHD Casson and Williamson fluids with cross diffusion, Journal of Molecular Liquids 233, 262–269, 2017.
23. O.K.Koriko, A.J.Omowaye, N.Sandeep, I.L.Animasaun, Analysis of boundary layer formed on an upper horizontal surface of a paraboloid of revolution within nanofluid flow in the presence of thermophoresis and Brownian motion of 29 nm, International Journal of Mechanical Sciences, 124-125, 22-36, 2017.

24. S.Saleem, M.Awais, S.Nadeem, N.Sandeep, T.Mustafa, Theoritical analysis of upper-convected Maxwell fluid flow with Cattaneo-Christov heat flux model, Chinese Journal of Physics, (In Press), 2017.
25. M. JayachandraBabu, N. Sandeep, MHD non-Newtonian fluid flow over a slendering stretching sheet in the presence of cross-diffusion effects, Alexandria Engineering Journal (2016) 55, 2193–2201.
26. M.Khader, A. M. Megahed, Numerical Solution for Boundary Layer Flow due to a Nonlinearly Stretching Sheet with Variable Thickness and Slip Velocity, The European Physical Journal Plus, 128 (2013) 100-108.
27. S. Pramanik, Casson fluid flow and heat transfer past an exponentially porous stretching surface in presence of thermal radiation, Ain Shams Engineering Journal, 5(1) (2014) 205-212.